AIChE WILEY InterScience DISCOVER SOMETHING GREAT

Experimental Investigation on Diesel PM Removal Using Uneven DBD Reactors

Shuiliang Yao, Kazuhiko Madokoro, Chihiro Fushimi, and Yuichi Fujioka
Chemical Research Group, Research Institute of Innovative Technology for the Earth, Kyoto 619-0292, Japan

DOI 10.1002/aic.11202
Published online May 14, 2007 in Wiley InterScience (www.interscience.wiley.com).

The removal of diesel particulate matter (PM) is experimentally carried out using two types of uneven dielectric barrier discharge (DBD) reactors driven by positive–negative pulse voltage power supplies. One uneven DBD reactor is fed with exhaust gases from a diesel engine at the exhaust gas temperature and another uneven DBD reactor is fed with PM dispersed in a gas mixture of oxygen and nitrogen at room temperature, where PM was collected from the exhaust gases of the diesel engine. PM emission rates, PM sizes, and PM oxidation products are measured using a PM emission rate monitor, a particle size spectrometer, and a gas chromatograph at various discharge energy densities. It has been found that most of PM is oxidized completely into gaseous products of CO and CO_2 under plasma discharge conditions. © 2007 American Institute of Chemical Engineers *AIChE J,* 53: 1891–1897, 2007
Keywords: diesel particulate matter, pulsed discharges, uneven DBD reactor, carbon oxidation

Introduction

In 1991, Harano et al. reported their study on soot oxidation in a silent discharge reactor.[1] They carried out the silent discharges at an electrical energy density as high as 5400 J/L; this high energy density suggested that PM removal using such a silent discharge would be expensive. Recently, the authors have developed an uneven dielectric barrier discharge (DBD) reactor driven by a pulse power supply for the removal of particulate matter (PM) emitted from a diesel engine.[2,3] The uneven DBD reactor was operated at an energy density as low as a value of 2–16 J/L. The energy efficiency (defined as the amount of removed PM per kW h electric power) of the DBD reactor achieved a level of 3–10.6 g/kWh, indicating that such a plasma PM removal method has potential for the practical use to remove PM from diesel engines. In order to make clear the reason why plasma PM removal using plasma discharges can be improved from an energy density of 5400 J/L to less than 20 J/L, it is important to know the mechanism of PM removal under pulsed plasma discharges. In 2000, Dorai et al. developed a quasihomogeneous gas-phase model to account for oxidation of soot particles and estimated the diameter changes when a pulsed corona discharge is used to generate reactive oxygen species, such as O, OH, and NO_2.[4] However, it is still unknown how PM is removed under plasma discharge conditions. In this study, we measure PM size changes and PM oxidation products due to plasma discharges generated using an uneven DBD reactor installed in the tail pipe of a diesel engine and using a model DBD reactor.

Correspondence concerning this article should be addressed to S. Yao at yao@rite.or.jp.

Experimental Methods

Figure 1 shows the experimental system including a hydro-dynamometer test cell, a discharge system for PM removal, PM emission monitor, and a particle size spectrometer. The hydro-dynamometer test cell consists of a 2-L diesel engine (Toyota, 4-cylinder, direct injection, 54 kW maximum power output at 4700 rpm), a system to control the diesel engine, and a performance measurement system of sensors to measure engine conditions such as fuel consumptions, rotation speeds, power outputs, exhaust gas flow rates, and pressures and temperatures of the exhaust gas from the diesel engine. The main properties of the diesel oil (Idemitsu Kosan) were specific gravity at 288 K: 0.827 g/cm^3; octane number: 56.7; flash point: 337.1 K; and sulfur: 0.0005 wt %. The diesel

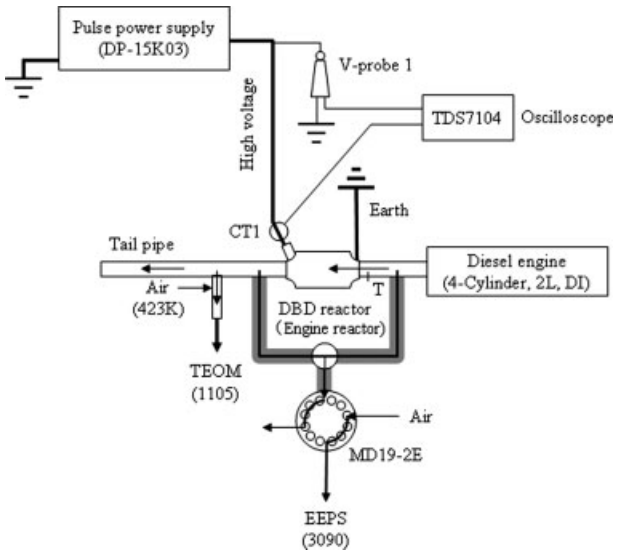

Figure 1. Experimental setup for plasma PM removal.

engine was operated at 1230 rpm and 3.1-kW power outputs, with an exhaust gas flow rate of 121 m^3/h (33.7 L/s) at atmospheric pressure and inlet temperature (430 K measured at point T in Figure 1). The exhaust gas composition was O_2: 15%, CO_2: 3.7%, H_2O: 3.7% (estimated as the same as CO_2), NO_2: 16 ppm, NO: 90 ppm, N_2: balance. The discharge system includes an uneven DBD reactor, a pulse power supply (DP-15K03, Peec), a voltage probe (V-probe 1, EP-50K, Peec), a current transformer (CT1, Model 2-1.0, Strangenes), and a digital phosphor oscilloscope (TDS 7104, Tektronix). The pulse power supply driven by a 12-V DC power supply (PQ15-80, Matsusada) was used to apply a positive–negative pulse voltage to the uneven DBD reactor. The voltage probe and current transformer were used to measure the output waveforms of voltage and current at high-voltage side, respectively. Typical waveforms of discharge voltage and current have been reported elsewhere.[3] The energy injection rate P_d (W) from the pulse power supply was calculated using Eq. 1 over one positive voltage pulse of one pulse repetition. One pulse repetition includes a pair of a positive voltage pulse and a negative voltage pulse. The energy injection over one positive voltage pulse is as the same as that over one negative voltage pulse:

$$P_d = 2F \sum_i [V_i I_i (t_{i+1} - t_i)] \quad (1)$$

where V_i and I_i are the pulse voltage (V) and the current (A) at the high-voltage side (CT1), respectively, at discharge time t_i (s); F is the pulse repetition (Hz).

The discharge energy injected into the DBD reactor per liter gas volume was defined as the energy density D_E in J/L using Eq. 2:

$$D_E = \frac{P_d}{V} \quad (2)$$

where V is the gas flow rate of the exhaust gases in L/min (33.7 L/s at 1 atm and 430 K), at which the residence time of the exhaust gases in the discharge zones of the DBD reactor is estimated to be 9.5 ms.

The uneven DBD reactor (engine reactor) was installed at the exhaust pipe line 1.5-m downstream of the exhaust outlet of the engine. This uneven DBD reactor was mainly made of 30 pairs of uneven alumina plates and uneven stainless steel (SUS) plates (Figure 2). The sizes of the main uneven alumina and SUS plates are given in detail in Figures 3A, B, respectively.

A part of the exhaust gas (0.2 L/min) from 0.05-m downstream of the uneven DBD reactor was diluted with air (2.3 L/min) at 423 K using a dilution unit. The air diluted exhaust gas was then sent to a PM mass monitor (TEOM 1105, Rupperecht & Patashnick) for PM emission rate measurement. PM removal X_w based on TEOM measurement was calculated using Eq. 3:

$$X_w = \frac{R_0 - R}{R_0} \times 100\% \quad (3)$$

where R_0 and R are PM emission rates (g/h) at the inlet and outlet of the DBD reactor, respectively.

For measuring sizes and numbers of PM sampled at the inlet or outlet of the DBD reactor, a particle size spectrometer (EEPS 3090,[5] from 5.6 to 560 nm, TSI) was installed. Before the PM size and number measurement, the sample gas was diluted 25 times with air at 423 K using a dilution unit (MD19-2E, Matter Engineering AG) and then diluted 6 times further with air at room temperature.

The PM removal X_i based on the EEPS measurements was calculated as follows:

$$X_i = \frac{[PM_i]_0 - [PM_i]}{[PM_i]_0} \times 100\% \quad (4)$$

where $[PM_i]_0$ and $[PM_i]$ are the concentrations (particles/cm^3) of PM with a PM size (diameter) d_i sampled at the inlet and outlet of the DBD reactor, respectively.

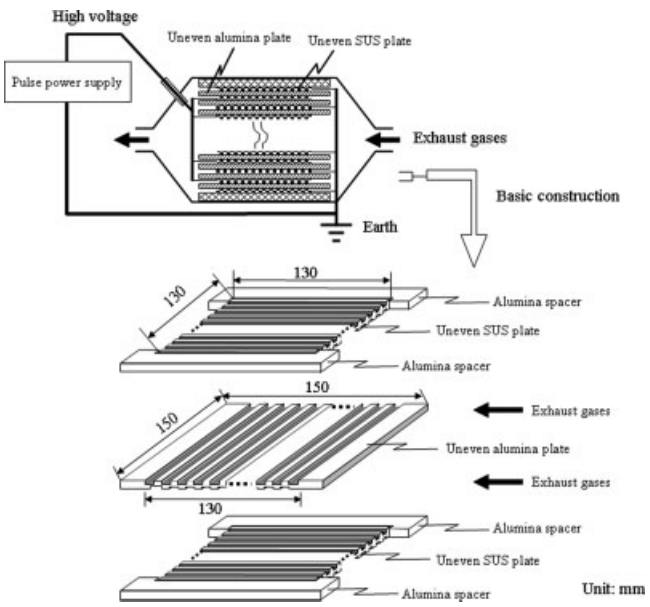

Figure 2. Assembly and the basic construction of the uneven DBD reactor.

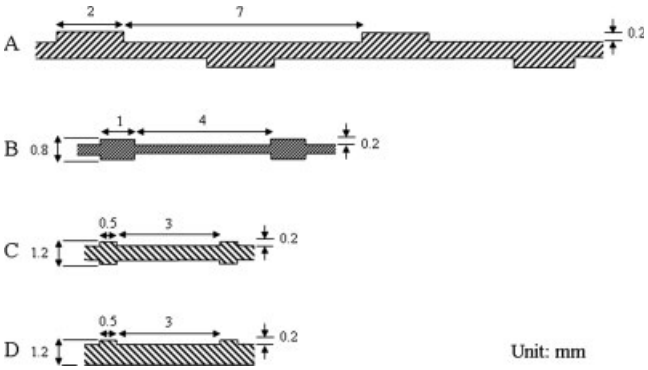

Figure 3. Side views and sizes of uneven alumina and stainless steel plates.

The PM removal efficiencies (A_{TEOM} and A_{EEPS}) were defined as grams of removed PM per kW h discharge power using Eqs. 5 and 6, respectively, where PM removals X_w and X_i are given in Eq. 3 based on TEOM measurement and in Eq. 4 based on EEPS measurement, respectively.

$$A_{TEOM} = \frac{R_0 X_w}{P_d \times 1000} \tag{5}$$

$$A_{EEPS} = \frac{R_0 X}{P_d \times 1000} \tag{6}$$

$$X = \frac{\sum_{t=1}^{n} [PM_i]_0 (d_i)^3 - \sum_{t=1}^{n} [PM_i](d_i)^3}{\sum_{t=1}^{n} [PM_i]_0 (d_i)^3} \times 100\% \tag{7}$$

where X in percentage is volumetric PM removal calculated on the inlet and outlet PM concentrations at various PM sizes (d_i).

In order to make sure whether and how many grams of PM are converted into CO and CO_2, another plasma PM removal system was assembled (Figure 4). PM containing gas was generated at a PM feeding rate of 3 mg/h using an atomizer (ATM 225,[6] Topas GmbH) to which a 3 L/min gas mixture of 2.4 L/min N_2 and 0.6 L/min O_2 was supplied; where PM was collected from the surfaces of the uneven alumina and stainless steel plates assembled in the DBD reactor under the aforementioned diesel engine conditions. PM was dispersed in water using an ultrasonic washer (US-1, Iuchi). The PM containing gas was further diluted with N_2 (3 L/min) and then supplied to a model reactor. The model reactor consisted of two uneven alumina plates (Figure 3A), one SUS plate (Figure 3C) connected to the high voltage output side of the pulse power supply, and two SUS plates (Figure 3D) used as the earth. Pulsed plasma discharges were carried out within the model reactor by applying pulse voltage from a pulse power supply. The pulse power supply (DP-10K5, Peec) was used to apply positive–negative voltage pulses to generate pulse corona discharges in the model reactor. The discharge voltage and anode current were measured using a voltage probe (V-probe 2, P6015A, Tektronix) and current transformer (CT2, P6021, Tektronix). The energy injection rate (in W) from the pulse power supply was calculated using Eq. 1.

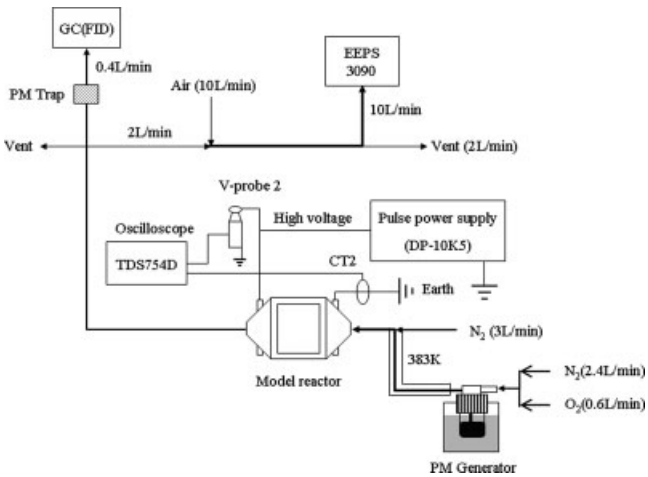

Figure 4. Experimental setup for plasma PM removal.

The gas mixture from the outlet of the model reactor was treated to remove PM and then analyzed using a gas chromatograph (GC) equipped with a 2-m Porapak-S column and a methanizer prior to hydrogen flame ion detector. A part of the gas mixture (2 L/min) from the model reactor was diluted with air (10 L/min) and sent to the particle size spectrometer. Only CO and CO_2 were found as the oxidation products of PM when pulse voltage was applied. From the concentrations of CO and CO_2, the amount of oxidized PM m (mg/h) was estimated using Eq. 8:

$$m = V_m \times ([CO] + [CO_2]) \times 60 \times 12 \times 1000 \tag{8}$$

where V_m is the flow rate of the gas mixture supplied to the model reactor (6 L/min at 1 atm and 298 K gas temperature at the inlet of the model reactor), at which the residence time of the gas mixture in the discharge zones of the model reactor is estimated to be 1.2 s. [CO] and [CO_2] are concentrations of CO and CO_2 (mol/L) in the exhaust gases from the model reactor, respectively. The numerical values of 60, 12, and 1000 are conversion factor of time from hour to minute, carbon molar weight, and conversion factor of carbon weight from gram to milligram, respectively.

The PM removal efficiency A_{GC} calculated on the base of gas chromatograph analysis was defined as Eq. 9:

$$A_{GC} = \frac{m}{P_d \times 1000} \tag{9}$$

Results and Discussion

PM removal using the engine reactor

Figure 5 shows a typical example of the concentrations of PM sampled at the inlet or the outlet of the DBD reactor at various elapsed times with or without plasma discharges. In the time range of 0–25 min, the PM concentrations sampled at the outlet of the DBD reactor are less than 10^4 particles/cm^3 at energy densities of 2.7, 2.0, and 2.8 J/L. The PM concentration sampled at the outlet of the DBD reactor at an energy density of 0 J/L (from time 25–30 min) is at a level of 6×10^4 particles/cm^3. The PM concentration sampled at the inlet of the DBD reactor from time 55–59 min is at a level of 6×10^4 particles/cm^3. The concentrations of PM sampled at the outlet of the DBD reactor are obviously lower than that sampled at the inlet of the DBD reactor. The con-

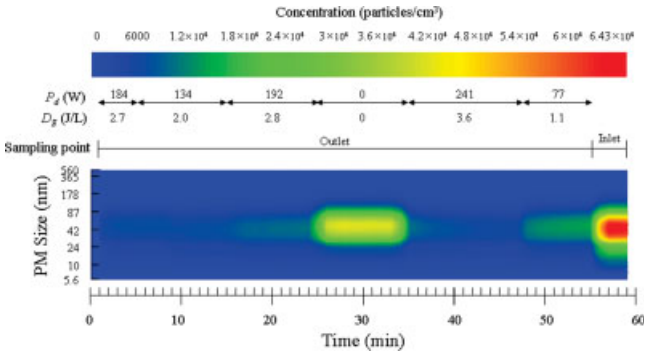

Figure 5. PM concentrations as a function of elapsed times at various energy injection rates and energy densities (engine reactor).

centrations of PM with plasma discharges (P_d or $D_E > 0$) are clearly lower than that without plasma discharges (including PM concentrations sampled at the outlet and inlet of the DBD reactor).

The concentrations of PM as a function of PM size at various energy densities are shown in Figure 6. At the inlet of the DBD reactor, the PM concentration peaked to a level of 6.3×10^4 particles/cm^3 at a PM size of 45.3 nm. The PM concentration at the outlet of the DBD reactor without plasma discharges (0 J/L in Figure 6) is less than that at the inlet of the DBD reactor, the difference in PM concentrations at the inlet and outlet of the DBD reactor is due to the adsorption of PM on the surfaces of alumina plates and stainless steel plates. The maximum PM concentrations are 1.34×10^4, 7.09×10^3, 9.34×10^3, and 7.14×10^3 particles/cm^3, respectively, at an energy density of 1.1, 2.0, 2.8, and 3.6 J/L; those PM concentrations are obviously lower than that at the inlet of the DBD reactor and that at the outlet of the DBD reactor without plasma discharges. These findings clearly show that PM is actually removed by plasma discharges.

The relative PM concentrations as a function of PM size at various energy densities are shown in Figure 7. The relative PM concentrations peaked in a PM size range of 39–52 nm. In a PM size range smaller than 22 nm, the relative PM concentrations at an energy density not less than 2.0 J/L are higher than that at an energy density lower than 2.0 J/L; this finding suggests that parts of PM of a diameter larger than 22 nm are not completely removed by oxidation/combustion to gaseous products or cannot be removed due to incombustible components such as metal oxides from lubricant oil, resulting in increasing in relative PM concentrations in a PM size range smaller than 22 nm.

Figure 8 shows the PM removal X_i as a function of PM size calculated using Eq. 4 at various energy densities. The PM removal X_i decreased to a minimum level at 107.5 nm and increased with increasing PM size without plasma discharges under which PM is removed by adsorption on the surfaces of alumina and stainless steel plates. PM removal X_i

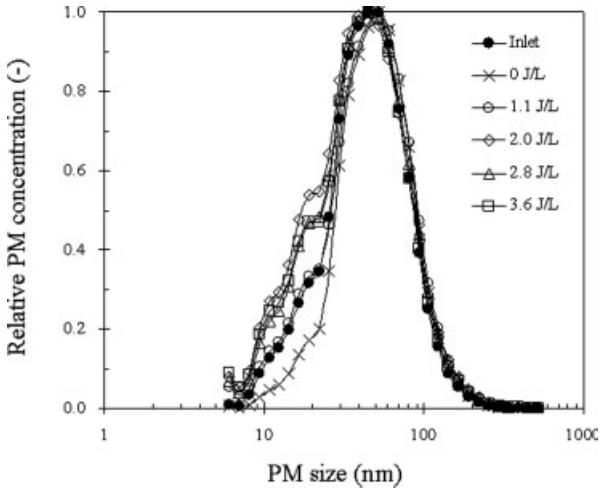

Figure 7. Relative PM concentrations as a function of PM size at various energy densities (engine reactor).

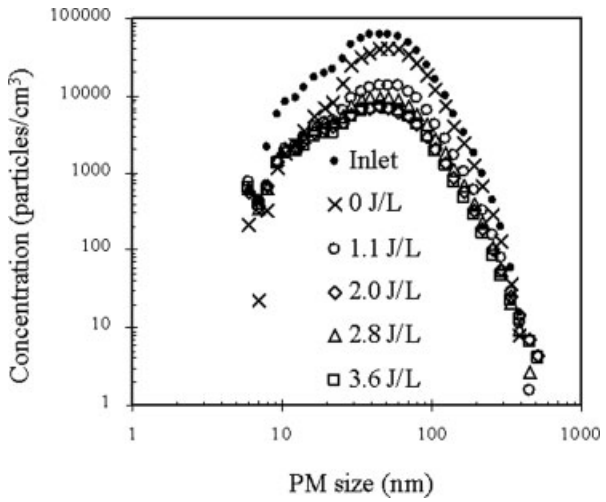

Figure 6. PM concentrations as a function of PM size at various energy densities (engine reactor).

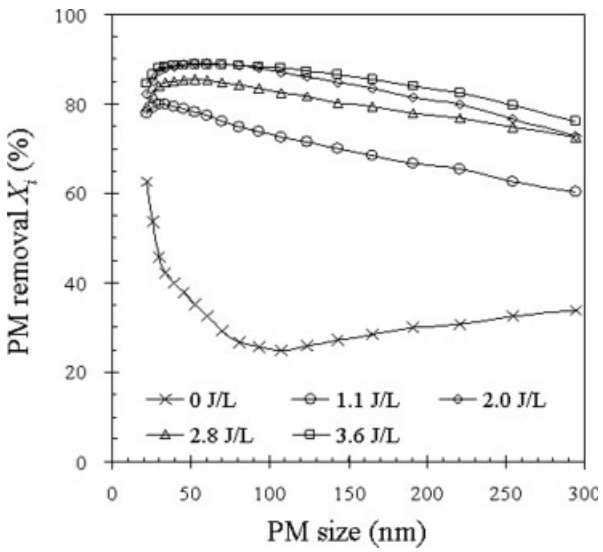

Figure 8. PM removals (X_i) as a function of PM size at various energy densities (engine reactor).

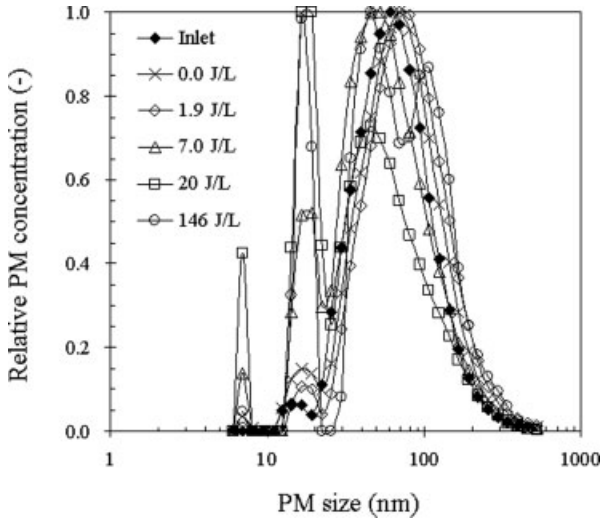

Figure 9. Relative PM concentrations as a function of PM size at various energy densities (model reactor).

increased with the increase in PM size and peaked at a PM size in 30–100 nm with plasma discharges. At an energy density of 1.1 J/L, the maximum PM removal was higher than 60% in PM size range of 30–300 nm. As no increase in PM size smaller than 52 nm of peak concentration was found, it is implied that PM is mainly removed by oxidation to gaseous products (CO and CO_2 as described later) resulting in the completed disappearance of solid PM.

The tendency of PM removal X_i with plasma discharges as a function of PM size is obviously different from that without plasma discharges (energy density 0.0 J/L). This difference is considerably due to the physical adsorption of PM on the surfaces of alumina and stainless steel plates and plasma-enhanced chemical oxidization/combustion of PM with oxygen species.

PM removal using the model reactor

PM removal X_i using the model reactor shown in Figure 4 was carried out. Figure 9 shows the relative PM concentration as a function of PM size at various energy densities. The peak values of the relative PM concentrations at the inlet of the DBD reactor were obtained at 60.4 and 16.5 nm in PM size ranges larger than 20 nm and smaller than 20 nm, respectively. The relative PM concentrations peaked at 69.8, 69.8, 52.3, 45.3, and 45.3 nm, respectively, at an energy density of 0.0, 1.9, 7.0, 20, and 146 J/L in a range of PM size larger than 20 nm. The relative PM concentrations in the PM size range of 12–22 nm and at 7.0 nm increased with increasing energy density; these increases in relative PM concentrations also suggested that parts of PM of a diameter larger than 22 nm are not completely removed by oxidation/combustion to gaseous products or cannot be removed due to incombustible components such as metal oxides from lubricant oil. The PM size at peak relative PM concentration as a function of energy density is shown in Figure 10. PM size decreased to 45.3 nm with the increase in energy density at energy densities higher than 1.9 J/L. This fact implied that the reduction of PM size is obviously due to the plasma discharges. In a PM size range between 10 and 20 nm, the relative PM concentration at energy densities of 20 and 146 J/L are remarkably higher than those at an energy density less than 20 J/L and at the inlet of the DBD reactor; the peak values of PM size increased from 16.5 nm at the inlet of the DBD reactor to 19.1 nm at the outlet of the DBD reactor and energy densities of 7.0 and 20 J/L. PM size is further reduced to 7.0 nm that can be observed in Figure 9. These findings suggested that PM size is reduced due to plasma discharges. However, the peak PM size did not decreased with increasing energy density at an energy density higher than 20 J/L.

For comparison, PM size changes using the engine reactor are also illustrated in Figure 10. Similar to those using the model DBD reactor, the PM sizes using the engine and model reactors at an energy density of 1.1 and 1.9 J/L are 52 and 70 nm, larger than 45 and 60 nm at the inlet of the engine and model reactors respectively; this fact indicated that PM became larger after passing through the DBD reactor possibly by agglomeration. The PM size is reduced to levels of 45.3 and 16.5 nm at an energy density higher than 20 J/L; those levels are as the same as that using the model DBD reactor. The reduction of PM size is due to the incomplete oxidation of PM. The decrease in peak PM concentration between the inlet and outlet (at 1.1 J/L) of the DBD reactor is 5×10^4 particles/cm^3, 77-fold higher than that of 5.6 nm at 1.1 J/L at the outlet of the DBD reactor (Figure 6); this fact suggested that the ratio of PM incomplete oxidation to PM complete oxidation is at a level of 1%.

Dorai et al. computed soot oxidation in the presence of NO and hydrocarbons at 453 K and atmospheric pressure.[4] They found that PM size and mass fraction are reduced in the pulsed corona discharges (energy density 38 J/L), respectively, from 100 to 60 nm and 1.0 to 0.21 after 0.2-s discharge times. The PM mass fraction loss is initiated by reactions with NO_2 which accounts for about 99.9% of the loss. Their findings suggested that the numbers of PM would be

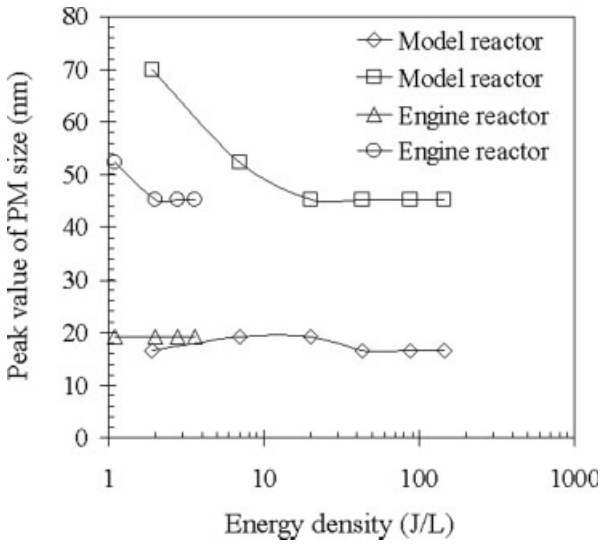

Figure 10. Peak PM sizes as a function of energy density at PM sizes higher or lower than 20 nm (model reactor).

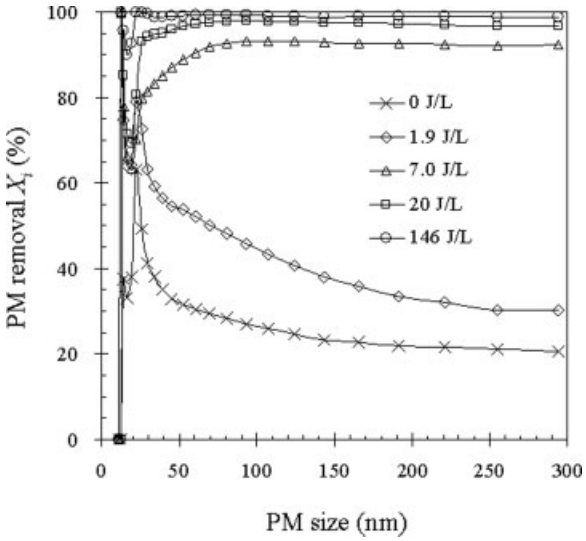

Figure 11. PM removals X_i as a function of PM size at various energy densities (model reactor).

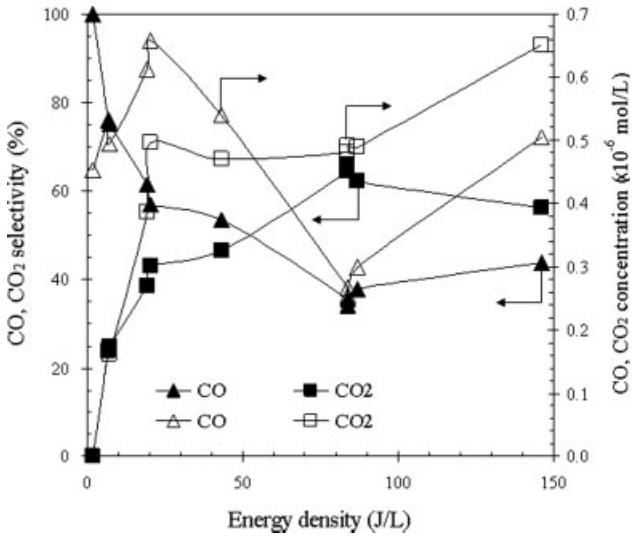

Figure 12. CO and CO_2 concentrations and selectivity at various energy densities (model reactor).

kept at a certain level if the PM is not completely oxidized when the discharge time is shorter than 0.2 s. However, our experiments showed that the PM removal in a PM size range of 10 nm to the peak PM size of 45–65 nm is as high as (1) 77% at energy density of 1.1 J/L using the engine reactor in Figure 7 and (2) 65% at an energy density of 7.0 J/L using the model DBD reactor in Figure 11. These facts suggested that PM oxidation in the plasma discharges are much faster than that calculated by Dorai et al.[4] The difference of PM oxidation rates between Dorai et al.'s simulation results and our experimental results may come from the oxidation temperature and other factors such as PM oxidation by ozone produced due to the plasma discharges. In Dorai et al.'s simulation, they used a constant temperature of 453 K; however, our newest experimental results showed that the gas temperature over the whole pulse discharge duration is not constant. For example, in a 6-μs pulsed air discharge duration using a DBD reactor, the gas temperature increases from the temperature of the background gases of 300–700 K, resulting in an increase in temperature as high as 400 K. If the temperature of the background gas is 453 K, its temperature would be elevated to 853 K at which the rate of PM oxidation by 11% oxygen is about 1000 times as high as that at 453 K based on our experimental results that will be presented elsewhere in near future.

The PM removal X_i calculated using Eq. 4 as a function of PM size between 10 and 300 nm is illustrated in Figure 11. PM removal decreased with increasing PM size without plasma discharges under which PM is removed by adsorption on the surfaces of alumina and stainless steel plates. PM removal also decreased with increasing PM size at an energy density of 1.9 J/L, the level of PM removal at 1.9 J/L is higher than that at 0.0 J/L. This finding indicated that PM is removed by both plasma-enhanced oxidation and adsorption on the surfaces of alumina and stainless steel plates. PM removal increased with the increase in PM size at energy densities of 7.0, 20, and 146 J/L. When PM size is larger than 20 nm, PM removal obviously increased with the increase in energy density.

The tendency of PM removals with and without plasma discharges is also different using the model reactor. This difference is also considerably due to the physical adsorption of PM on the surfaces of alumina and stainless steel plates under conditions without plasma discharges and plasma-enhanced chemical oxidization/combustion of PM with oxygen species.

As the main component of PM is carbon, the oxidation products were found to be CO and CO_2 only. The concentration and selectivity of CO and CO_2 are shown in Figure 12. The concentration and selectivity of CO decreased and those of CO_2 increased with increasing energy density. CO selectivity is higher that CO_2 at an energy density less than 50 J/L, but lower than that of CO_2 at an energy density higher than 50 J/L. From the facts that high CO_2 selectivity was

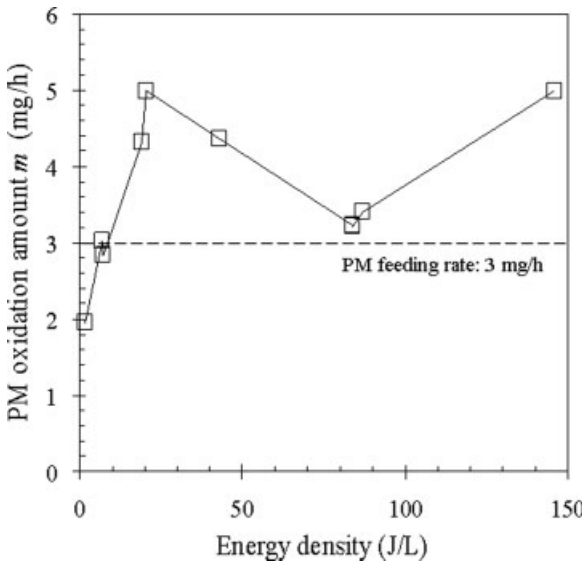

Figure 13. PM removal abilities m at various energy densities (model reactor).

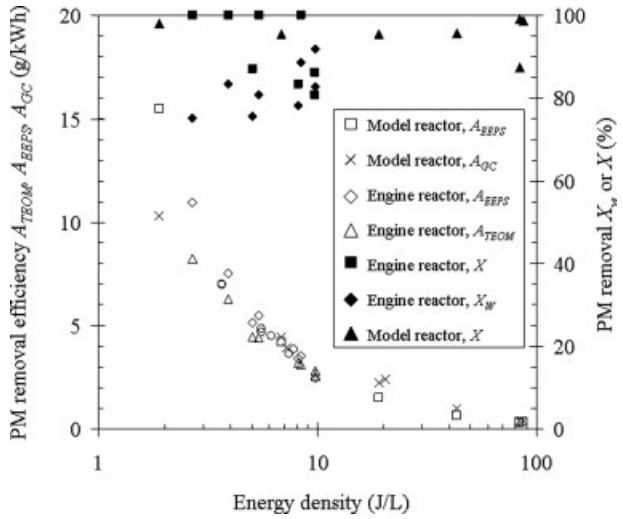

Figure 14. PM removal efficiencies and PM removals as a function of energy density (engine and model reactors).

found at a high energy density and higher concentrations of active oxygen species, such as O, OH, NO_2, and O_3, can be produced at a higher energy density, active oxygen species may promote PM and CO oxidation to CO_2.

In order to estimate the PM removal ability using the model DBD reactor, the PM removal ability calculated using Eq. 8 as a function of energy density is shown in Figure 13. The PM removal ability at an energy density higher than 12 J/L is higher than that of PM feeding rate (3 mg/h), implying that under such conditions (room temperature, 6 L/min gas flow rate, O_2 10%), PM can be removed completely. The PM removal ability higher than 3 mg/h is due to the oxidation of PM accumulated on the surfaces of the alumina and stainless steel plates by adsorption.

The PM removal efficiencies of A_{TEOM}, A_{EEPS}, and A_{GC} calculated using Eqs. 5, 6, and 9 are shown in Figure 14 together with PM removals (X_{w} and X). All PM removal efficiencies of A_{TEOM}, A_{EEPS}, and A_{GC} decreased with increasing energy density. No obvious difference was found in the PM removal efficiencies of A_{TEOM}, A_{EEPS}, and A_{GC} except that at 1.9 J/L. As PM removal efficiencies of A_{TEOM}, A_{EEPS}, and A_{GC} were given by measurements, respectively, using TEOM (PM weight emission rates), EEPS (PM sizes and concentrations), and GC (gaseous PM oxidation products), results in Figure 14 implied EEPS and GC are usable for the measurement of PM removal efficiency. Furthermore, as PM removal efficiencies of A_{TEOM}, A_{EEPS}, and A_{GC} were obtained under conditions of engine exhaust gases (430 K) and synthesized PM gas (room temperature), results in Figure 14 also suggested that the temperature difference between 298 and 430 K does not influence PM removal efficiency.

PM removal X_{w} (engine reactor) using the DBD reactor installed in the tail pipe of the engine increased with increasing energy density with a range of 75–92% based on the TEOM measurements. PM removal X (engine reactor) also using the DBD reactor installed in the tail pipe of the engine is within a range of 80–100% based on the EEPS measurements. PM removal X (model reactor) using the DBD reactor supplied with the synthesized PM gases changes within 85–98% based on the EEPS measurements. Generally, PM removals of X_{w} and X are higher than 75% under all experiment conditions with plasma discharges.

Conclusions

PM removal using two types of uneven DBD reactors was investigated. The main conclusions are summarized as follows:

1. Most of solid PM is completely oxidized to gaseous products of CO and CO_2 if PM oxidation starts under plasma discharge conditions. CO selectivity decreased and CO_2 selectivity increased with increasing energy density. A small part of PM remains with a reduced size due to incomplete oxidation. The ratio of PM incomplete oxidation to PM complete oxidation is estimated to be at a level of 1% when the engine reactor is used.
2. PM of 10–300 nm can be adsorbed on the surfaces of alumina and stainless steel plates of the DBD reactor if pulsed voltage is not applied for plasma discharges. The PM removal by adsorption is different from that by plasma discharges.
3. PM removal efficiency decreased from 16 to 0.34 g/kW h with the increase in energy density; PM removal (X_{w} and X) is in the range of 75–100%.
4. PM removal efficiencies using the engine reactor at 430 K and model reactor at room temperature are almost the same, indicating these two temperatures do not influence PM removal.

Acknowledgments

A part of this manuscript has been presented at the 72nd Annual Meeting of The Society of Chemical Engineers, Japan (Kyoto, March 2007).

This work was supported by the New Energy and Industrial Technology Development Organization, Japan. Prof. Yoshimasa Nihei at Tokyo University of Science and Dr. Hirohisa Tanaka at Daihatsu Motor Co. Ltd. are thanked for useful discussions.

Literature Cited

1. Harano A, Sadakata M, Sato M. Soot oxidation in a silent discharge. *J Chem Eng Jpn.* 1991;24:100–106.
2. Yao S, Okumoto M, Madokoro K, Yashima T, Suzuki E. Pulsed dielectric barrier discharge reactor for diesel particulate matter removal. *AIChE J.* 2004;50(8):1901–1907.
3. Yao S, Fushimi C, Madokoro K, Yamada K. Uneven dielectric barrier discharge reactors for diesel particulate matter removal. *Plasma Chem Plasma Process.* 2006;26:481–493.
4. Dorai R, Hassouni H, Kushner MJ. Interaction between soot particles and NO_x during dielectric barrier discharge plasma remediation of simulated diesel exhaust. *J Appl Phys.* 2000;88:6060–6071.
5. Burtscher H. Physical characterization of particulate emission from diesel Engines, a review. *Aerosol Sci.* 2005;36:896–932.
6. Kinney PD, Pui DYH, Mulholland GW, Bryner NP. Use of the electrostatic classification method to size 0.1 μm SRM particles—a feasibility study. *J Res Nat Inst Standards Technol.* 2001;96(2):147–176.

Manuscript received Jan. 11, 2007, and revision received Mar. 22, 2007.